

Instant Extraction of Non-Perturbative Tripartite Entanglement

Diana Méndez Avalos,^{1,*} Kensuke Gallock-Yoshimura,^{2,†} Laura J. Henderson,^{2,3,‡} and Robert B. Mann^{2,3,§}

¹ *Centro de Nanociencias y Nanotecnología Universidad Nacional Autónoma de México (CNyN-UNAM) Km 107 Carretera Tijuana-Ensenada, C.P. 22800, Ensenada, B.C. Mexico*

² *Department of Physics and Astronomy, University of Waterloo, Waterloo, Ontario, N2L 3G1, Canada*

³ *Institute for Quantum Computing, University of Waterloo, Ontario, N2L 3G1, Canada*

We consider the problem of extracting tripartite entanglement through single local instantaneous interactions of a separable target system A-B-C with a scalar field. We find, non-perturbatively, that tripartite entanglement is easily extracted in this scenario, in strong contrast to bipartite extraction, which is not possible due to a no-go theorem. The tripartite entanglement is of the GHZ-type, and an optimal value of the coupling exists that admits maximal extraction.

Introduction The entanglement of quantum fields has been an area of significant attention over the past few decades, with areas of interest in quantum information [1, 2] and metrology [3], quantum energy teleportation [4, 5], the AdS/CFT correspondence [6], black hole entropy [7, 8] and the black hole information paradox [9–15].

The entanglement present in the vacuum state of a quantum field was originally shown by Valentini [16] and later by Reznik *et. al.* [17] to be able to be swapped to a pair first-quantised particle detectors, even if the two detectors are not in causal contact throughout the duration of the interaction. The extracted entanglement was subsequently shown to be distillable into Bell pairs [18]. Since then, there has been a significant amount of research [19–33] investigating the process of entangling a pair of two-level particle detectors, known as Unruh-DeWitt (UDW) detectors [34, 35], through localised, time dependent interactions with the vacuum state of quantum scalar field. This process has become to be known as *entanglement harvesting* [36].

The process of swapping field entanglement to particle detectors is not limited to bipartite entanglement, but can be extended to multipartite entanglement as well, of which much less is known. Silman and Reznik demonstrated that a finite-duration interaction of N UDW detectors with the vacuum of a scalar field yields a reduced density matrix containing N -partite entanglement between the detectors that can in principle be distilled to that of a W -state [37]. Some time later Lorek *et. al.* used Gaussian quantum mechanics to show that three harmonic oscillators in a $(1+1)$ -dimensional cavity can extract genuine tripartite entanglement following interaction with the scalar field vacuum state even if the detectors remained spacelike separated [38]. Furthermore, they found that in this context it was easier to harvest tripartite entanglement than bipartite entanglement. More recently, it was shown using perturbation theory that three initially uncorrelated UDW detectors in $(3+1)$ -dimensional Minkowski space are able to harvest tripartite entanglement from the scalar field. Outside of the context of entanglement harvesting, it was found that acceleration leads to a degradation in the tripartite en-

tanglement of initially entangled detectors [39, 40].

A nonperturbative calculation of the final state of the three detectors following the interaction with field can be carried out by assuming the detectors couple instantaneously with the field, which is modelled using Dirac-delta switching. If each detector couples only once to the field with delta-switching, bipartite entanglement harvesting has been shown to be impossible [25]: at least one detector will need to couple twice [26] or the the detectors must switch in a temporal superposition [41]. More recently it has been shown that a third party, with a detector that also couples to the field with delta-switching, is able to prevent any bipartite correlations from forming between the two detectors [42], indicating the existence of multipartite entanglement between the three parties.

Here we demonstrate that harvesting tripartite entanglement with delta-switching is considerably easier than the bipartite case: we can nonperturbatively extract genuine tripartite entanglement when each of the detectors switches only once. This is in striking contrast with the bipartite case, where at least one detector must switch more than once to allow for any entanglement between the detector pair. An optimal value of the coupling exists for maximally harvesting the tripartite entanglement, which is of the GHZ-type, having no residual bipartite entanglement upon tracing over any one of the three detectors.

Harvesting Protocol Consider three static UDW detectors $A, B,$ and C in an $(n+1)$ -dimensional Minkowski spacetime. Each detector $D \in \{A, B, C\}$ has a spatial shape specified by a smearing function $F_D(\mathbf{x} - \mathbf{x}_D) \in \mathbb{R}$, where \mathbf{x}_D is the position of center of mass, and instantaneously locally interacts with a quantum scalar field $\hat{\phi}(\mathbf{x})$ via the interaction Hamiltonian

$$\hat{H}_I(t) = \sum_{D \in \{A, B, C\}} \lambda_D \eta_D \delta(t - T_D) \hat{\mu}_D(t) \otimes \int d^n x F_D(\mathbf{x} - \mathbf{x}_D) \hat{\phi}(\mathbf{x}(t)). \quad (1)$$

that we refer to as delta-switching [25]. Here λ_D is the coupling constant, $\eta_D \delta(t - T_D)$ is the delta switching with

a strength η_D and T_D is the time when detector- D interacts with the field. $\hat{\mu}_D(t)$ is the monopole moment of detector- D , which acts on different Hilbert spaces depending on D . For instance, $\hat{\mu}_A(t) = \hat{m}_A(t) \otimes \mathbf{1}_B \otimes \mathbf{1}_C$, and similarly for detectors B and C , where

$$\hat{m}_D(t) = e^{i\Omega_D t} |1_D\rangle \langle 0_D| + e^{-i\Omega_D t} |0_D\rangle \langle 1_D|, \quad (2)$$

with detector- D 's ground $|0_D\rangle$ and excited $|1_D\rangle$ states, and an energy gap $\Omega_D \in \mathbb{R}$ between them.

Without loss of generality, we assume that the detectors turn on in the following order

$$T_A \leq T_B \leq T_C \quad (3)$$

in which case the time-evolution operator in the interaction picture $\hat{U}_I = \mathcal{T} \exp \left[-i \int_{\mathbb{R}} dt \hat{H}_I(t) \right]$ (with \mathcal{T} the time-ordering symbol) is nonperturbatively given by

$$\hat{U}_I = e^{[\hat{\mu}_C(T_C) \otimes \hat{Y}_C(T_C)]} e^{[\hat{\mu}_B(T_B) \otimes \hat{Y}_B(T_B)]} e^{[\hat{\mu}_A(T_A) \otimes \hat{Y}_A(T_A)]} \quad (4)$$

where

$$\hat{Y}_D(t) := -i\lambda_D \eta_D \int d^n x F_D(\mathbf{x} - \mathbf{x}_D) \hat{\phi}(\mathbf{x}(t)) \quad (5)$$

is the smeared field operator at detector D 's location.

We next introduce two quantities

$$\Theta_{D,E} := -i \langle 0 | [\hat{Y}_D(T_D), \hat{Y}_E(T_E)] | 0 \rangle \quad (6)$$

$$\omega_{D,E} := \frac{1}{2} \langle 0 | \{ \hat{Y}_D(T_D), \hat{Y}_E(T_E) \} | 0 \rangle \quad (7)$$

which are respectively the vacuum expectation values of the commutator, $\Theta_{D,E}$, and anticommutator, $\omega_{D,E}$ for $D, E \in \{A, B, C\}$ with $D \neq E$.

If two detectors are causally disconnected then $\Theta_{D,E} = 0$ and they cannot communicate. The anticommutator $\omega_{D,E}$, on the other hand, is nonzero even when detectors cannot send and receive signals. In fact, the extracted entanglement using causally disconnected detectors directly comes from $\omega_{D,E}$ [43].

Suppose the field is massless and the initial state of the total system is

$$\hat{\rho}_0 = |0_A 0_B 0_C\rangle \langle 0_A 0_B 0_C| \otimes |0\rangle \langle 0|, \quad (8)$$

where $|0\rangle$ is the Minkowski vacuum state of the field. The final state $\hat{\rho}_{ABC}$ of the detectors can be obtained by tracing out the field degrees of freedom of the final state of the system: $\text{Tr}_\phi[\hat{U}_I \hat{\rho}_0 \hat{U}_I^\dagger]$. The density matrix $\hat{\rho}_{ABC}$ in the basis $\{|0_A 0_B 0_C\rangle, |0_A 0_B 1_C\rangle, |0_A 1_B 0_C\rangle, |1_A 0_B 0_C\rangle, |0_A 1_B 1_C\rangle, |1_A 0_B 1_C\rangle, |1_A 1_B 0_C\rangle, |1_A 1_B 1_C\rangle\}$ can be writ-

ten as (see Supplementary Material for the derivation)

$$\hat{\rho}_{ABC} = \begin{bmatrix} r_{11} & 0 & 0 & 0 & r_{15} & r_{16} & r_{17} & 0 \\ 0 & r_{22} & r_{23} & r_{24} & 0 & 0 & 0 & r_{28} \\ 0 & r_{23}^* & r_{33} & r_{34} & 0 & 0 & 0 & r_{38} \\ 0 & r_{24}^* & r_{34}^* & r_{44} & 0 & 0 & 0 & r_{48} \\ r_{15}^* & 0 & 0 & 0 & r_{55} & r_{56} & r_{57} & 0 \\ r_{16}^* & 0 & 0 & 0 & r_{56}^* & r_{66} & r_{67} & 0 \\ r_{17}^* & 0 & 0 & 0 & r_{57}^* & r_{67}^* & r_{77} & 0 \\ 0 & r_{28}^* & r_{38}^* & r_{48}^* & 0 & 0 & 0 & r_{88} \end{bmatrix} \quad (9)$$

where the matrix elements $r_{i,j}$ are functions of the quantities

$$f_D = \exp \left(-\frac{1}{2} \int d^n k |\beta_D(\mathbf{k})|^2 \right), \quad (10a)$$

$$\Theta_{D,E} = i \int d^n k \left(\beta_D^*(\mathbf{k}) \beta_E(\mathbf{k}) - \beta_D(\mathbf{k}) \beta_E^*(\mathbf{k}) \right), \quad (10b)$$

$$\omega_{D,E} = -\frac{1}{2} \int d^n k \left(\beta_D^*(\mathbf{k}) \beta_E(\mathbf{k}) + \beta_D(\mathbf{k}) \beta_E^*(\mathbf{k}) \right), \quad (10c)$$

$$\beta_D(\mathbf{k}) := -\frac{i\lambda_D \eta_D}{2\sqrt{2|\mathbf{k}|}} \tilde{F}_D^*(\mathbf{k}) e^{i(|\mathbf{k}|T_D - \mathbf{k} \cdot \mathbf{x}_D)}, \quad (10d)$$

and where

$$\tilde{F}_D(\mathbf{k}) = \int \frac{d^n x}{\sqrt{(2\pi)^n}} F_D(\mathbf{x}) e^{i\mathbf{k} \cdot \mathbf{x}} \quad (11)$$

is the Fourier transform of the smearing function, $F_D(\mathbf{x})$. Once the shape of detectors $F_D(\mathbf{x})$ is specified, we can calculate each element in the density matrix.

With the density matrix of the final state of the three detectors fully calculated, we will now consider the resulting tripartite entanglement between the three detectors. We choose the π -tangle as our measure of tripartite entanglement [44], which puts a lower bound on the genuine tripartite entanglement in the mixed state $\hat{\rho}_{ABC}$. It is defined as

$$\pi := \frac{1}{3} (\pi_A + \pi_B + \pi_C) \quad (12)$$

with

$$\pi_A := \mathcal{N}_{A(BC)}^2 - \mathcal{N}_{A(B)}^2 - \mathcal{N}_{A(C)}^2 \quad (13)$$

and similarly for subsystems B and C . The negativities of the subsystems are

$$\mathcal{N}_{A(BC)} := \|\hat{\rho}_{ABC}^{T_A}\| - 1 \quad (14)$$

$$\mathcal{N}_{A(B)} := \|(\text{Tr}_C[\hat{\rho}_{ABC}])^{T_A}\| - 1 \quad (15)$$

where T_A is the partial transpose with respect to detector A and $\|\cdot\|$ is the trace norm, with similar definitions for detectors B and C . We will refer to these as the tripartite and bipartite negativity respectively. In all scenarios we consider the no-go theorem [25] ensures

the latter quantity is zero, and so the π -tangle provides a measure of genuine tripartite entanglement.

Instant Tripartite entanglement harvesting We will now calculate the π -tangle of three identical detectors in $(3+1)$ -dimensional Minkowski spacetime so that the switching strength η , coupling constant, λ , and energy gap Ω are the same for each. The latter assumption is not required since the elements of the density matrix only depend on the gap via phases, which cancel out if the detectors switch only once.

We shall take the Gaussian smearing function

$$F_D(\mathbf{x}) = \exp\left(-\frac{(\mathbf{x} - \mathbf{x}_D)^2}{2\sigma^2}\right), \quad (16)$$

with characteristic width σ to describe the shape of each detector, allowing for exact computation of f_D from (10).

First, as shown in Fig. 1(a), we will consider a configuration where the three detectors are placed at the vertices of an equilateral triangle with side length L , coupling to the field at times $T_A = 0$, $T_B = T$ and $T_C = 2T$. We plot the π -tangle of this configuration as a function of T and L for $\lambda = 10$ in Fig. 2. We see that the three detector system has genuine tripartite entanglement, after each detector couples to the field just once through delta-switching. This is in contrast to bipartite entanglement between any two detectors, which is forbidden by the no-go theorem[25].

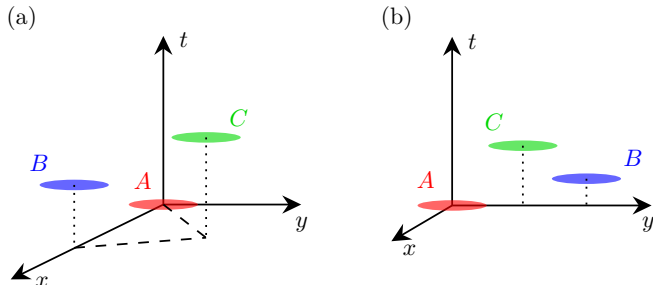


FIG. 1 Spacetime diagram illustrating (a) the triangle configuration, and (b) the line configuration.

The positive π -tangle is strictly a result of the positive tripartite negativities $\mathcal{N}_{A(BC)}$ and $\mathcal{N}_{B(AC)}$, as shown in Fig. 3. In other words, detector A is entangled with the (BC) subsystem and detector B is entangled with the (AC) subsystem. However, detector C is not entangled with the (AB) subsystem. We also confirm that that the bipartite negativities between the detectors are zero (as required by the no-go theorem[25]), meaning no pair of detectors are entangled. Consequently, the tripartite entanglement is of the GHZ-type and not of the W-type.

As expected, a third detector cannot be used to avoid the no-go theorem since the coupling of the third detector will act as a displacement operator on the field, moving it into a coherent state [25].

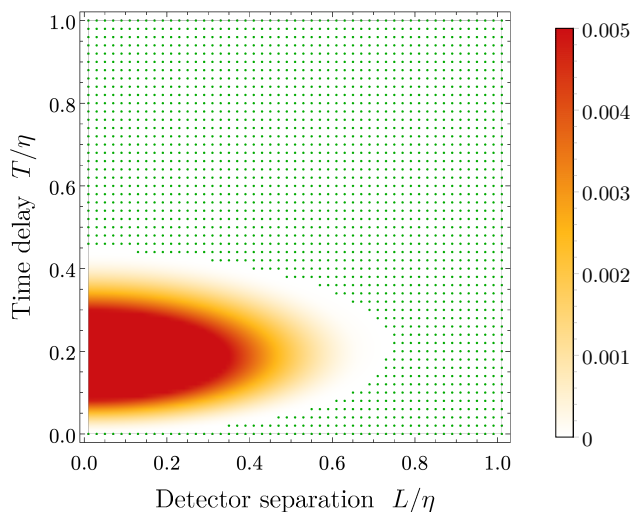


FIG. 2 The π -tangle as a function of the side length, L , and time delay, T , for three detectors arranged in an equilateral triangle that each couple to the field once with Dirac δ switching. The detectors have an energy gap $\Omega\eta = 1$, width $\sigma = \eta$, and coupling $\lambda = 10$. The green dots indicate the regions of the parameter space where the π -tangle is zero.

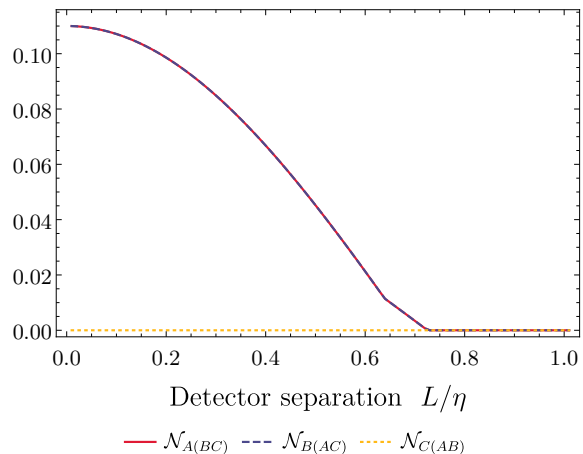


FIG. 3 The tripartite negativities as a function of the side length, L , for three detectors arranged in an equilateral triangle that each couple to the field once with Dirac delta-switching. Two of the three tripartite negativities are non-zero (and equal), which results in a positive π -tangle. All of the bipartite negativities are zero. The time between switches is $T = 0.25\eta$, the detectors have an energy gap of $\Omega\eta = 1$, width $\sigma = \eta$ and coupling $\lambda = 10$.

The non-zero tripartite entanglement can be better understood by interpreting it from the perspective of subsystems. The negativity $\mathcal{N}_{A(BC)}$ quantifies the entanglement between detector A with the subsystem (BC) . From this perspective, the first subsystem A switches once, and then the second subsystem (BC) switches twice, once at the location of detector B and once at the location of detector C . This type of switching is analo-

gous to the BAA-type switching described in [26], which is complex enough to allow the two systems to become entangled. Similarly, the negativity $\mathcal{N}_{B(AC)}$ quantifies the entanglement between detector B and the subsystem (AC) . The switching order (Eq. (3)) means that the first subsystem (AC) interacts with the field (at the location of detector A), then the second subsystem B interacts with the field, and finally the first subsystem interacts again with the field (at the location of detector C), which is analogous to the ABA-type switching that also allows for the systems to become entangled. Following this logic, the negativity $\mathcal{N}_{C(AB)}$, quantifies the entanglement between the subsystem (AB) and detector C . The switching order of these systems is analogous to the AAB-type switching, which prohibits the systems from becoming entangled.

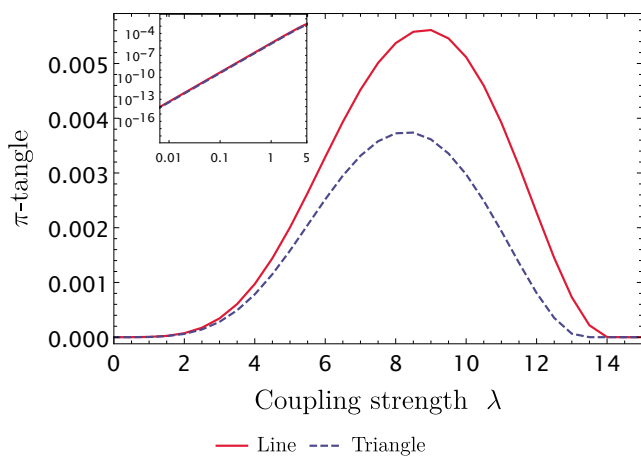


FIG. 4 A comparison of the π -tangle for three detectors arranged in an equilateral triangle with side length $L = 0.4\eta$ and in a line of length $L_{AB} = 0.4\eta$ that each couple to the field once with Dirac delta-switching as a function of the coupling strength, λ . The time between switches is $T = 0.25\eta$ and the detectors have an energy gap of $\Omega\eta = 1$ and a width of $\sigma = \eta$.

In Fig. 4, we compare the equilateral triangle configuration [Fig. 1(a)] with one where the detectors are arranged in a straight line with detector C in the middle [Fig. 1(b)], equidistant from detectors A and B . Setting the distance between detectors A and B on the line to equal the side length of the equilateral triangle, we find that the π -tangle is significantly larger in the case of the line for all values of the coupling constant where tripartite entanglement harvesting is possible. Furthermore, the π -tangle is non-zero for larger values of the coupling constant in the linear configuration.

Both of these effects are due to the reduced distance between detector C and the other two detectors in the line configuration as opposed to the triangle. The reduced distance means there is stronger signaling between detector C and detectors A and B , which leads to an increase in the resulting tripartite entanglement in the

linear configuration. We have checked this over a broad range of separations and time delays and found this general trend to hold. More explicitly, the final state of the three detector system depends on the quantities (Eq. (10)) which only depend on the relative spacetime positions of at most two detectors, and so the overall configuration of the detectors only matters insofar as it changes their relative pairwise distances.

We also find that the qualitative behaviour of the π -tangle as a function of the coupling strength is the same. When the coupling strength is small ($\lambda \lesssim 5$), the π -tangle has quartic growth with increasing λ as shown in the inset of Fig. 4. In this regime, the evolution of the detectors, and hence their final state, $\hat{\rho}_{ABC}$, can be described as a perturbative expansion in even powers of the coupling strength. Hence to lowest order, the matrix elements and π -tangle will respectively be quadratic and quartic in λ . As the coupling constant increases out of the perturbative regime, the π -tangle reaches a maximum and then falls off exponentially to zero. In other words, there is an optimal value of λ for maximally harvesting tripartite entanglement. We have checked this for other configurations and find it to be a general feature.

Finally, we explore the effects of signaling on the tripartite entanglement. We first note that when two detectors switch at the same time, the commutator $\Theta_{A,B} = 0$, so they do not signal to each other. We find in this case that three detectors can still have a positive π -tangle even if detectors A and B do not signal to each other; however the both must be able to signal to detector C . This is illustrated in Fig. 5, where for the linear configuration (Fig. 1(b)), with $T_A = T_B = 0$ and the distance between detectors A and B fixed to $L_{AB} = 2.8\eta$, we plot the π -tangle as a function of $T_C \geq 0$ and L_{AC} . We observe that the π -tangle is positive only when detector C is between A and B ($L_{AC} < L_{BC}$) and that it is maximum on the overlapping lightcones of detectors A and B . In other words, the π -tangle will be maximized if detector C is positioned so that it maximizes its communication with both detectors A and B . Furthermore the π -tangle is zero when detector C is outside of the light code of only one of detectors A or B , we conclude that the C must be able to communicate with both detectors in order for them to become tripartite entangled.

Reversing the situation so that the first detector A switches followed by detectors B and C switching simultaneously, the π -tangle remains zero, which further illustrates that entanglement is only possible if the first two detectors are able to communicate with the third.

We emphasize that despite a significant amount of overlap in the smearing functions, the two detectors do not communicate since $\Theta_{AB} = 0$. Indeed, when the smearing function of the detectors has a standard deviation of $\sigma = \eta$, if the distance between detectors A and B is increased beyond $L_{AB} = 2.8\eta$, the π -tangle will be zero for the region of parameter space we explored.

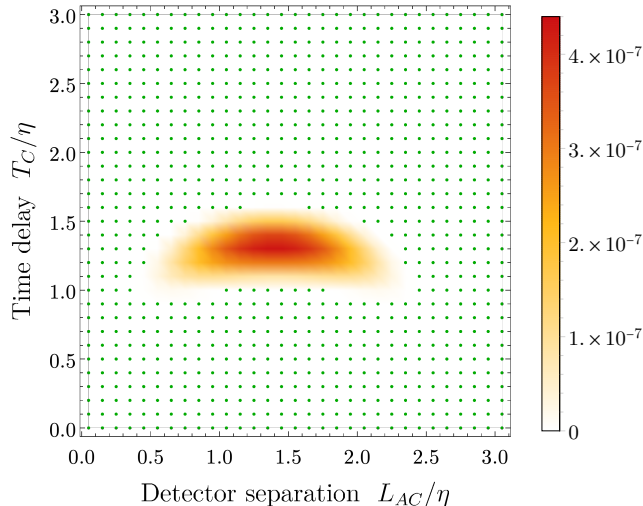


FIG. 5 The π -tangle for three detectors arranged in a line that each couple to the field once with Dirac δ switching as a function of switching time of detector C and the distance of detector C from A . Detector A and B switch at $T_A = T_B = 0$ and are separated by a distance of $L_{AB} = 2.8\eta$. The detectors have an energy gap of $\Omega\eta = 1$ and a width of $\sigma = \eta$ and the coupling constant is $\lambda = 2.5$. The green dots indicate the regions of the parameter space where the π -tangle is zero.

Conclusion In strong contrast to the bipartite case, harvesting tripartite entanglement is possible with a single instantaneous switch of each detector. The absence of any bipartite negativity implies the 3-detector system has harvested genuine GHZ-type tripartite entanglement following the interaction, rather than W-type entanglement. Moreover, it is possible to harvest tripartite entanglement even if the first two detectors that switch cannot communicate, provided both detectors are able to communicate with last detector. This is quite unlike the case of two detectors (with three switchings), where communication between the detectors is required.

All of the above indicates that it is easier to harvest tripartite entanglement than bipartite entanglement, commensurate with earlier work in $(1+1)$ dimensions [38], since there are looser constraints on the communication between the detectors.

Our results are also compatible with requirement that in order for two detectors to become entangled with delta switching, at least one must couple to the field twice [26]. Since the π -tangle depends on the entanglement between one detector and the subsystem consisting of the other two (averaged over all three combinations), we can interpret the resulting tripartite entanglement by noting that the two-detector subsystem always interacts with the field twice. From this perspective, it is not surprising that it can become entangled with the remaining detector, provided that it is not the last to interact.

Our approach for tripartite entanglement harvesting can be extended to harvesting N -partite entanglement using N detectors in a straightforward way, allowing one to probe N -point correlations in a quantum field. It can also be extended to many of the same problems that were explored in the bipartite case. The effects of spacetime curvature and event horizons are of particular interest. The entanglement structure of a quantum field on a black hole spacetime [27, 31, 45] induces several new effects, including entanglement shadows in the vicinity of the black hole, and entanglement amplification if the black hole rotates. It would be interesting to see the extent to which such effects are present in the multipartite case.

Acknowledgements This work was supported in part by the Natural Science and Engineering Research Council of Canada and by Asian Office of Aerospace Research and Development Grant No. FA2386-19-1-4077.

* g7_menav18@ens.cnyu.unam.mx

† Electronic address: kgallock@uwaterloo.ca

‡ l7henderson@uwaterloo.ca

§ rbmann@uwaterloo.ca

- [1] A. Peres and D. R. Terno, *Rev. Mod. Phys.* **76**, 93 (2004), URL <https://link.aps.org/doi/10.1103/RevModPhys.76.93>.
- [2] L. Lamata, M. A. Martin-Delgado, and E. Solano, *Phys. Rev. Lett.* **97**, 250502 (2006), URL <https://link.aps.org/doi/10.1103/PhysRevLett.97.250502>.
- [3] T. C. Ralph, G. J. Milburn, and T. Downes, *Phys. Rev. A* **79**, 022121 (2009), URL <https://link.aps.org/doi/10.1103/PhysRevA.79.022121>.
- [4] M. Hotta, *Journal of the Physical Society of Japan* **78**, 034001 (2009), <https://doi.org/10.1143/JPSJ.78.034001>, URL <https://doi.org/10.1143/JPSJ.78.034001>.
- [5] M. Hotta, arXiv preprint arXiv:1101.3954 (2011).
- [6] S. Ryu and T. Takayanagi, *Phys. Rev. Lett.* **96**, 181602 (2006), hep-th/0603001.
- [7] S. N. Solodukhin, *Living Reviews in Relativity* **14**, 8 (2011), 1104.3712.
- [8] R. Brustein, M. B. Einhorn, and A. Yarom, *JHEP* **01**, 098 (2006), hep-th/0508217.
- [9] J. Preskill, in *International Symposium on Black holes, Membranes, Wormholes and Superstrings Woodlands, Texas, January 16-18, 1992* (1992), pp. 22–39, hep-th/9209058.
- [10] S. D. Mathur, *Class.Quant.Grav.* **26**, 224001 (2009), 0909.1038.
- [11] A. Almheiri, D. Marolf, J. Polchinski, and J. Sully, *Journal of High Energy Physics* **2013**, 62 (2013), ISSN 1029-8479, URL [https://doi.org/10.1007/JHEP02\(2013\)062](https://doi.org/10.1007/JHEP02(2013)062).
- [12] S. L. Braunstein, S. Pirandola, and K. Życzkowski, *Phys. Rev. Lett.* **110**, 101301 (2013), 0907.1190.
- [13] R. B. Mann, *Black Holes: Thermodynamics, Information, and Firewalls*, SpringerBriefs in Physics (Springer, 2015), ISBN 9783319144955, 9783319144962.

- [14] J. Louko, J. High Energ. Phys. **2014**, 142 (2014), URL [https://doi.org/10.1007/JHEP09\(2014\)142](https://doi.org/10.1007/JHEP09(2014)142).
- [15] S. Luo, H. Stoltenberg, and A. Albrecht, Phys. Rev. D **95**, 064039 (2017), URL <https://link.aps.org/doi/10.1103/PhysRevD.95.064039>.
- [16] A. Valentini, Phys. Lett. A **153**, 321 (1991), ISSN 0375-9601, URL <http://www.sciencedirect.com/science/article/pii/0375960191909525>.
- [17] B. Reznik, Found. Phys. **33**, 167 (2003), URL <https://doi.org/10.1023/A:1022875910744>.
- [18] B. Reznik, A. Retzker, and J. Silman, Phys. Rev. A **71**, 042104 (2005), URL <https://link.aps.org/doi/10.1103/PhysRevA.71.042104>.
- [19] G. V. Steeg and N. C. Menicucci, Phys. Rev. D **79**, 044027 (2009), URL <https://link.aps.org/doi/10.1103/PhysRevD.79.044027>.
- [20] S. J. Olson and T. C. Ralph, Phys. Rev. A **85**, 012306 (2012), URL <https://link.aps.org/doi/10.1103/PhysRevA.85.012306>.
- [21] A. Pozas-Kerstjens and E. Martín-Martínez, Phys. Rev. D **92**, 064042 (2015), URL <https://link.aps.org/doi/10.1103/PhysRevD.92.064042>.
- [22] E. Martín-Martínez, A. R. H. Smith, and D. R. Terno, Phys. Rev. D **93**, 044001 (2016), URL <https://link.aps.org/doi/10.1103/PhysRevD.93.044001>.
- [23] E. Martín-Martínez and B. C. Sanders, New Journal of Physics **18**, 043031 (2016), ISSN 1367-2630, URL <http://dx.doi.org/10.1088/1367-2630/18/4/043031>.
- [24] S. Kukita and Y. Nambu, Entropy **19**, 449 (2017), ISSN 1099-4300, URL <http://dx.doi.org/10.3390/e19090449>.
- [25] P. Simidzija and E. Martín-Martínez, Phys. Rev. D **96**, 065008 (2017), URL <https://link.aps.org/doi/10.1103/PhysRevD.96.065008>.
- [26] P. Simidzija, R. H. Jonsson, and E. Martín-Martínez, Phys. Rev. D **97**, 125002 (2018), URL <https://link.aps.org/doi/10.1103/PhysRevD.97.125002>.
- [27] L. J. Henderson, R. A. Hennigar, R. B. Mann, A. R. H. Smith, and J. Zhang, Class. Quantum Gravity **35** (2018), URL <https://doi.org/10.1088/2F1361-6382%2Faae27e>.
- [28] K. K. Ng, R. B. Mann, and E. Martín-Martínez, Phys. Rev. D **98**, 125005 (2018), URL <https://link.aps.org/doi/10.1103/PhysRevD.98.125005>.
- [29] L. J. Henderson, R. A. Hennigar, R. B. Mann, A. R. Smith, and J. Zhang, J. High Energ. Phys. **2019**, 178 (2019).
- [30] W. Cong, E. Tjoa, and R. B. Mann, J. High Energ. Phys. **2019**, 21 (2019).
- [31] E. Tjoa and R. B. Mann, Journal of High Energy Physics **2020**, 1 (2020).
- [32] W. Cong, C. Qian, M. R. Good, and R. B. Mann, Journal of High Energy Physics **2020**, 67 (2020), ISSN 1029-8479, URL [https://doi.org/10.1007/JHEP10\(2020\)067](https://doi.org/10.1007/JHEP10(2020)067).
- [33] Q. Xu, S. A. Ahmad, and A. R. H. Smith (2020), Arxiv:2006.11301v1, URL <http://arxiv.org/abs/2006.11301>.
- [34] W. G. Unruh, Phys. Rev. D **14**, 870 (1976), URL <https://link.aps.org/doi/10.1103/PhysRevD.14.870>.
- [35] B. S. DeWitt, in *General Relativity: An Einstein centenary survey*, edited by S. W. Hawking and W. Israel (1979), pp. 680–745.
- [36] G. Salton, R. B. Mann, and N. C. Menicucci, New J. Phys. **17**, 035001 (2015).
- [37] J. Silman and B. Reznik, Phys. Rev. A **71**, 054301 (2005), URL <https://link.aps.org/doi/10.1103/PhysRevA.71.054301>.
- [38] K. Lorek, D. Pecak, E. G. Brown, and A. Dragan, Phys. Rev. A **90**, 032316 (2014), URL <https://link.aps.org/doi/10.1103/PhysRevA.90.032316>.
- [39] M.-R. Hwang, D. Park, and E. Jung, Phys. Rev. A **83**, 012111 (2011), URL <https://link.aps.org/doi/10.1103/PhysRevA.83.012111>.
- [40] J. Szypulski, P. Grochowski, K. Dębski, and A. Dragan (2021).
- [41] L. J. Henderson, A. Belenchia, E. Castro-Ruiz, C. Budroni, M. Zych, i. c. v. Brukner, and R. B. Mann, Phys. Rev. Lett. **125**, 131602 (2020), URL <https://link.aps.org/doi/10.1103/PhysRevLett.125.131602>.
- [42] A. Sahu, I. Melgarejo-Lermas, and E. Martín-Martínez, Phys. Rev. D **105**, 065011 (2022), URL <https://link.aps.org/doi/10.1103/PhysRevD.105.065011>.
- [43] E. Tjoa and E. Martín-Martínez, Phys. Rev. D **104**, 125005 (2021), URL <https://link.aps.org/doi/10.1103/PhysRevD.104.125005>.
- [44] Y.-C. Ou and H. Fan, Phys. Rev. A **75**, 062308 (2007), URL <https://link.aps.org/doi/10.1103/PhysRevA.75.062308>.
- [45] M. P. G. Robbins, L. J. Henderson, and R. B. Mann, Class. Quant. Grav. **39**, 02LT01 (2022), 2010.14517.

Supplementary Material

Reduced Density Matrix of the Detectors

Here we show how the reduced density matrix (9) is computed.

Using

$$\exp \left[\hat{\mu}_D(T_D) \otimes \hat{Y}_D(T_D) \right] = \mathbb{1}_D \otimes \cosh(\hat{Y}_D(T_D)) + \hat{\mu}_D(T_D) \otimes \sinh(\hat{Y}_D(T_D)), \quad (17)$$

the nonperturbative expression (4) the time evolution operator can be expanded as

$$\begin{aligned} \hat{U}_I &= \left(\mathbb{1}_A \otimes \mathbb{1}_B \otimes \mathbb{1}_C \otimes \cosh \hat{Y}_C + \mathbb{1}_A \otimes \mathbb{1}_B \otimes \hat{m}_C(T_C) \otimes \sinh \hat{Y}_C \right) \\ &\quad \times \left(\mathbb{1}_A \otimes \mathbb{1}_B \otimes \mathbb{1}_C \otimes \cosh \hat{Y}_B + \mathbb{1}_A \otimes \hat{m}_B(T_B) \otimes \mathbb{1}_C \otimes \sinh \hat{Y}_B \right) \\ &\quad \times \left(\mathbb{1}_A \otimes \mathbb{1}_B \otimes \mathbb{1}_C \otimes \cosh \hat{Y}_A + \hat{m}_A(T_A) \otimes \mathbb{1}_B \otimes \mathbb{1}_C \otimes \sinh \hat{Y}_A \right), \end{aligned} \quad (18)$$

where we use the shorthand $\hat{Y}_D := \hat{Y}_D(T_D)$. This can be further simplified by using the identities $\cosh \hat{Y}_D = (e^{\hat{Y}_D} + e^{-\hat{Y}_D})/2$ and $\sinh \hat{Y}_D = (e^{\hat{Y}_D} - e^{-\hat{Y}_D})/2$ and noting that each term in Eq. (18) can be written as

$$(\hat{m}_A(T_A))^{(1-z)/2} \otimes (\hat{m}_B(T_B))^{(1-y)/2} (\hat{m}_C(T_C))^{(1-x)/2} \otimes \hat{X}_{(x,y,z)} \quad (19)$$

for $x, y, z \in \{1, -1\}$ and where

$$\hat{X}_{(x,y,z)} := \frac{1}{2^3} \left(e^{\hat{Y}_C} + x e^{-\hat{Y}_C} \right) \left(e^{\hat{Y}_B} + y e^{-\hat{Y}_B} \right) \left(e^{\hat{Y}_A} + z e^{-\hat{Y}_A} \right). \quad (20)$$

Therefore we have

$$\hat{U}_I = \sum_{x,y,z} (\hat{m}_A(T_A))^{(1-z)/2} \otimes (\hat{m}_B(T_B))^{(1-y)/2} \otimes (\hat{m}_C(T_C))^{(1-x)/2} \otimes \hat{X}_{(x,y,z)}. \quad (21)$$

When the operator \hat{U}_I is applied to the initial state of the detectors $|0_A 0_B 0_C\rangle$, the resulting state is

$$\begin{aligned} &\hat{U}_I |0_A 0_B 0_C\rangle \\ &= \left(\sum_{x,y,z} (\hat{m}_A(T_A))^{(1-z)/2} (\hat{m}_B(T_B))^{(1-y)/2} \otimes (\hat{m}_C(T_C))^{(1-x)/2} \otimes \hat{X}_{(x,y,z)} \right) |0_A 0_B 0_C\rangle \\ &= \sum_{x,y,z} \left(e^{i\Omega_A T_A} \right)^{(1-z)/2} \left(e^{i\Omega_B T_B} \right)^{(1-y)/2} \left(e^{i\Omega_C T_C} \right)^{(1-x)/2} \left| \left(\frac{1-z}{2} \right)_A \left(\frac{1-y}{2} \right)_B \left(\frac{1-x}{2} \right)_C \right\rangle \otimes \hat{X}_{(x,y,z)}. \end{aligned} \quad (22)$$

From this, the reduced density matrix $\hat{\rho}_{ABC}$ is obtained by tracing over the field

$$\begin{aligned} \hat{\rho}_{ABC} &= \text{Tr}_\phi [\hat{U}_I \hat{\rho}_0 \hat{U}_I^\dagger] \\ &= \sum_{\substack{x,y,z \\ q,r,s}} \left[e^{i(1-z)\Omega_A T_A/2} e^{i(1-y)\Omega_B T_B/2} e^{i(1-x)\Omega_C T_C/2} e^{-i(1-s)\Omega_A T_A/2} e^{-i(1-r)\Omega_B T_B/2} e^{-i(1-q)\Omega_C T_C/2} \right. \\ &\quad \left. \times \left\langle 0 \left| \hat{X}_{(q,r,s)}^\dagger \hat{X}_{(x,y,z)} \right| 0 \right\rangle \left| \left(\frac{1-z}{2} \right)_A \left(\frac{1-y}{2} \right)_B \left(\frac{1-x}{2} \right)_C \right\rangle \left\langle \left(\frac{1-s}{2} \right)_A \left(\frac{1-r}{2} \right)_B \left(\frac{1-q}{2} \right)_C \right| \right], \end{aligned} \quad (23)$$

using the fact that the smeared field is anti-Hermitian, $\hat{Y}_D^\dagger = -\hat{Y}_D$.

To obtain the final expression (9), let us focus on $\langle 0 | \hat{X}_{(q,r,s)}^\dagger \hat{X}_{(x,y,z)} | 0 \rangle$. Using the result [25]

$$\left\langle 0 \left| e^{u\hat{Y}_D + v\hat{Y}_E} \right| 0 \right\rangle = \exp \left(-\frac{1}{2} \int d^n \mathbf{k} |u\beta_D(\mathbf{k}) + v\beta_E(\mathbf{k})|^2 \right), \quad (24)$$

for $u, v \in \mathbb{C}$ and $\beta_D(\mathbf{k})$ defined in (10d), we employ the Baker-Campbell-Hausdorff formula to obtain

$$\begin{aligned}
& \left\langle 0 \left| \hat{X}_{(q,r,s)}^\dagger \hat{X}_{(x,y,z)} \right| 0 \right\rangle \\
&= \frac{1}{2^6} \left\langle 0 \left| \left(e^{-\hat{Y}_A} + s e^{\hat{Y}_A} \right) \left(e^{-\hat{Y}_B} + r e^{\hat{Y}_B} \right) \left(e^{-\hat{Y}_C} + q e^{\hat{Y}_C} \right) \left(e^{\hat{Y}_C} + x e^{-\hat{Y}_C} \right) \left(e^{\hat{Y}_B} + y e^{-\hat{Y}_B} \right) \left(e^{\hat{Y}_A} + z e^{-\hat{Y}_A} \right) \right| 0 \right\rangle \\
&= \frac{1}{64} \sum_{\substack{a,b,c \\ j,k,\ell}} s^{(1+a)/2} r^{(1+b)/2} q^{(1+c)/2} x^{(1-j)/2} y^{(1-k)/2} z^{(1-\ell)/2} \left\langle 0 \left| e^{a\hat{Y}_A} e^{b\hat{Y}_B} e^{c\hat{Y}_C} e^{j\hat{Y}_C} e^{k\hat{Y}_B} e^{\ell\hat{Y}_A} \right| 0 \right\rangle \\
&= \frac{1}{64} \sum_{\substack{a,b,c \\ j,k,\ell}} s^{(1+a)/2} r^{(1+b)/2} q^{(1+c)/2} x^{(1-j)/2} y^{(1-k)/2} z^{(1-\ell)/2} \left(f_A^{(a+\ell)^2} f_B^{(b+k)^2} f_C^{(c+j)^2} e^{(a+\ell)(b+k)\omega_{A,B}} e^{(a+\ell)(c+j)\omega_{A,C}} \right. \\
&\quad \left. \times e^{(b+k)(c+j)\omega_{B,C}} e^{i/2(a-\ell)(b+k)\Theta_{A,B}} e^{i/2(a-\ell)(c+j)\Theta_{A,C}} e^{i/2(b-k)(c+j)\Theta_{B,C}} \right) \tag{25}
\end{aligned}$$

for $a, b, c, j, k, \ell \in \{-1, +1\}$ and where f_D , $\Theta_{D,E}$ and $\omega_{D,E}$ are defined in equation 10.

Finally, we arrive at the expression for the density matrix describing the final state of the three detectors:

$$\begin{aligned}
\hat{\rho}_{ABC} &= \frac{1}{64} \sum_{\substack{x,y,z \\ q,r,s}} \left[e^{i(1-z)\Omega_A T_A/2} e^{i(1-y)\Omega_B T_B/2} e^{i(1-x)\Omega_C T_C/2} e^{-i(1-s)\Omega_A T_A/2} e^{-i(1-r)\Omega_B T_B/2} e^{-i(1-q)\Omega_C T_C/2} \right. \\
&\quad \times \sum_{\substack{a,b,c \\ j,k,\ell}} \left(s^{(1+a)/2} r^{(1+b)/2} q^{(1+c)/2} x^{(1-j)/2} y^{(1-k)/2} z^{(1-\ell)/2} f_A^{(a+\ell)^2} f_B^{(b+k)^2} f_C^{(c+j)^2} e^{(a+\ell)(b+k)\omega_{A,B}} \right. \\
&\quad \left. \times e^{(a+\ell)(c+j)\omega_{A,C}} e^{(b+k)(c+j)\omega_{B,C}} e^{i/2(a-\ell)(b+k)\Theta_{A,B}} e^{i/2(a-\ell)(c+j)\Theta_{A,C}} e^{i/2(b-k)(c+j)\Theta_{B,C}} \right) \\
&\quad \left. \times \left| \left(\frac{1-z}{2} \right)_A \left(\frac{1-y}{2} \right)_B \left(\frac{1-x}{2} \right)_C \right\rangle \left\langle \left(\frac{1-s}{2} \right)_A \left(\frac{1-r}{2} \right)_B \left(\frac{1-q}{2} \right)_C \right| \right] \tag{26}
\end{aligned}$$

where $a, b, c, j, k, \ell, q, r, s, x, y, z \in \{-1, +1\}$. Evaluating the sums results the density matrix (9), where the individual elements can be read off in the basis $\{|0_A 0_B 0_C\rangle, |0_A 0_B 1_C\rangle, |0_A 1_B 0_C\rangle, |1_A 0_B 0_C\rangle, |0_A 1_B 1_C\rangle, |1_A 0_B 1_C\rangle, |1_A 1_B 0_C\rangle, |1_A 1_B 1_C\rangle\}$. For completeness, we have included some of the elements of the density matrix (9):

$$\begin{aligned}
r_{11} &= \frac{1}{8} \left(1 + f_A^4 + f_B^4 \cos(2\Theta_{AB}) + f_A^4 f_B^4 \cosh(4\omega_{AB}) \right. \\
&\quad + f_C^4 \cos(2\Theta_{AC}) \cos(2\Theta_{BC}) + f_A^4 f_C^4 \cos(2\Theta_{BC}) \cosh(4\omega_{AC}) \\
&\quad + f_B^4 f_C^4 \left[\cos(2\Theta_{AB}) \cos(2\Theta_{AC}) \cosh(4\omega_{BC}) - \sin(2\Theta_{AB}) \sin(2\Theta_{AC}) \sinh(4\omega_{BC}) \right] \\
&\quad \left. + f_A^4 f_B^4 f_C^4 \left[\cosh(4\omega_{AC}) \cosh(4\omega_{BC}) \cosh(4\omega_{AB}) + \sinh(4\omega_{AC}) \sinh(4\omega_{BC}) \sinh(4\omega_{AB}) \right] \right), \tag{27a}
\end{aligned}$$

$$\begin{aligned}
r_{22} &= \frac{1}{8} \left(1 + f_A^4 + f_B^4 \cos(2\Theta_{AB}) + f_A^4 f_B^4 \cosh(4\omega_{AB}) \right. \\
&\quad - f_C^4 \cos(2\Theta_{AC}) \cos(2\Theta_{BC}) - f_A^4 f_C^4 \cos(2\Theta_{BC}) \cosh(4\omega_{AC}) \\
&\quad - f_B^4 f_C^4 \left[\cos(2\Theta_{AB}) \cos(2\Theta_{AC}) \cosh(4\omega_{BC}) - \sin(2\Theta_{AB}) \sin(2\Theta_{AC}) \sinh(4\omega_{BC}) \right] \\
&\quad \left. - f_A^4 f_B^4 f_C^4 \left[\cosh(4\omega_{AC}) \cosh(4\omega_{BC}) \cosh(4\omega_{AB}) + \sinh(4\omega_{AC}) \sinh(4\omega_{BC}) \sinh(4\omega_{AB}) \right] \right), \tag{27b}
\end{aligned}$$

$$\begin{aligned}
r_{15} &= \frac{1}{8} e^{-i(\Omega_B T_B + \Omega_C T_C)} f_C^4 \left(i \cos(2\Theta_{AC}) \sin(2\Theta_{BC}) + i f_A^4 \cosh(4\omega_{AC}) \sin(2\Theta_{BC}) \right. \\
&\quad + f_B^4 \left[\cos(2\Theta_{AB}) \cos(2\Theta_{AC}) \sinh(4\omega_{BC}) - \sin(2\Theta_{AB}) \sin(2\Theta_{AC}) \cosh(4\omega_{BC}) \right] \\
&\quad \left. + f_A^4 f_B^4 \left[\cosh(4\omega_{BC}) \sinh(4\omega_{AB}) \sinh(4\omega_{AC}) + \sinh(4\omega_{BC}) \cosh(4\omega_{AB}) \cosh(4\omega_{AC}) \right] \right), \tag{27c}
\end{aligned}$$

and the remaining elements can be similarly found from Eq. (26).